

M Protein and Hyaluronic Acid Capsule Are Essential for *In Vivo* Selection of *covRS* Mutations Characteristic of Invasive Serotype M1T1 Group A *Streptococcus*

Jason N. Cole,^{a,b} Morgan A. Pence,^a Maren von Köckritz-Blickwede,^a Andrew Hollands,^a Richard L. Gallo,^{a,c,d} Mark J. Walker,^b and Victor Nizet^{a,e,f}

Department of Pediatrics, University of California San Diego, La Jolla, California, USA^a; School of Chemistry and Molecular Biosciences, The University of Queensland, St. Lucia, Queensland, Australia^b; Department of Medicine, University of California San Diego, La Jolla, California, USA^c; Veterans Affairs San Diego Healthcare Center, San Diego, California, USA^d; Skaggs School of Pharmacy and Pharmaceutical Sciences, University of California San Diego, La Jolla, California, USA^e; and Rady Children's Hospital, San Diego, California, USA^f

ABSTRACT The initiation of hyperinvasive disease in group A *Streptococcus* (GAS) serotype M1T1 occurs by mutation within the *covRS* two-component regulon (named *covRS* for control of virulence regulatory sensor kinase), which promotes resistance to neutrophil-mediated killing through the upregulation of bacteriophage-encoded Sda1 DNase. To determine whether other virulence factors contribute to this phase-switching phenomenon, we studied a panel of 10 isogenic GAS serotype M1T1 virulence gene knockout mutants. While loss of several individual virulence factors did not prevent GAS *covRS* switching *in vivo*, we found that M1 protein and hyaluronic acid capsule are indispensable for the switching phenotype, a phenomenon previously attributed uniquely to the Sda1 DNase. We demonstrate that like M1 protein and Sda1, capsule expression enhances survival of GAS serotype M1T1 within neutrophil extracellular traps. Furthermore, capsule shares with M1 protein a role in GAS resistance to human cathelicidin antimicrobial peptide LL-37. We conclude that a quorum of GAS serotype M1T1 virulence genes with cooperative roles in resistance to neutrophil extracellular killing is essential for the switch to a hyperinvasive phenotype *in vivo*.

IMPORTANCE The pathogen group A *Streptococcus* (GAS) causes a wide range of human infections ranging from the superficial “strep throat” to potentially life-threatening conditions, such as necrotizing fasciitis, also known as “flesh-eating disease.” A marked increase in the number of cases of severe invasive GAS infection during the last 30 years has been traced to the emergence and spread of a single clone of the M1T1 serotype. Recent studies have shown that GAS serotype M1T1 bacteria undergo a genetic “switch” *in vivo* to a hypervirulent state that allows dissemination into the bloodstream. The present study was undertaken to identify specific GAS serotype M1T1 virulence factors required for this switch to hypervirulence. The surface-anchored GAS M1 protein and hyaluronic acid capsule are found to be essential for the switching phenotype, and a novel role for capsule in GAS resistance to host defense peptides and neutrophil extracellular killing is revealed.

Received 16 July 2010 Accepted 29 July 2010 Published 31 August 2010

Citation Cole, J. N., M. A. Pence, M. von Köckritz-Blickwede, A. Hollands, R. L. Gallo, et al. 2010. M protein and hyaluronic acid capsule are essential for *in vivo* selection of *covRS* mutations characteristic of invasive serotype M1T1 group A *Streptococcus*. *mBio* 1(4):e00191-10. doi:10.1128/mBio.00191-10.

Invited Editor Anna Norrby-Teglund, Karolinska Institute **Editor** Donald Low, Mt. Sinai Hospital

Copyright © 2010 Cole et al. This is an open-access article distributed under the terms of the Creative Commons Attribution-Noncommercial-Share Alike 3.0 Unported License, which permits unrestricted noncommercial use, distribution, and reproduction in any medium, provided the original author and source are credited.

Address correspondence to Victor Nizet, vnizet@ucsd.edu.

Streptococcus pyogenes (group A *Streptococcus* [GAS]) is an important bacterial pathogen responsible for numerous human diseases, ranging from benign skin infections, such as impetigo and pharyngitis, to life-threatening invasive conditions, including necrotizing fasciitis and toxic shock syndrome (1, 2). The globally disseminated GAS serotype M1T1 clone is chiefly responsible for the resurgence of severe invasive disease caused by GAS over the past 3 decades (3). Recent evidence indicates that invasive disease caused by serotype M1T1 GAS is instigated by spontaneous mutation of the *covRS* two-component regulator (4–6), which results in the upregulation of several virulence factors, including a bacteriophage-encoded DNase designated Sda1 (5). High-level expression of Sda1 facilitates the degradation of DNA neutrophil extracellular traps (NETs), thereby promoting GAS resistance to neutrophil-mediated killing at the initial site of infection (7, 8).

Concomitantly, *covRS* mutation blocks expression of streptococcal pyrogenic exotoxin B (SpeB), a broad-spectrum GAS cysteine protease (5, 9), thereby preserving the integrity of Sda1 and several additional GAS virulence proteins (10). SpeB inactivation allows streptokinase, M1 protein, and host plasminogen to remain intact at the site of infection, leading to accumulation of plasmin activity on the bacterial cell surface and facilitating systemic spread (11).

Targeted deletion of *sda1* abolishes selection for *covRS* mutation *in vivo* following subcutaneous mouse infection, identifying Sda1 as a pivotal factor in invasive disease caused by GAS serotype M1T1 (6). This finding suggests that selective pressure exerted by neutrophils, and in particular NETs, during local infection favors accumulation of SpeB-negative *covRS* mutants within the GAS serotype M1T1 population, thereby enhancing the propensity for severe invasive disease (6). The objective of the current investiga-

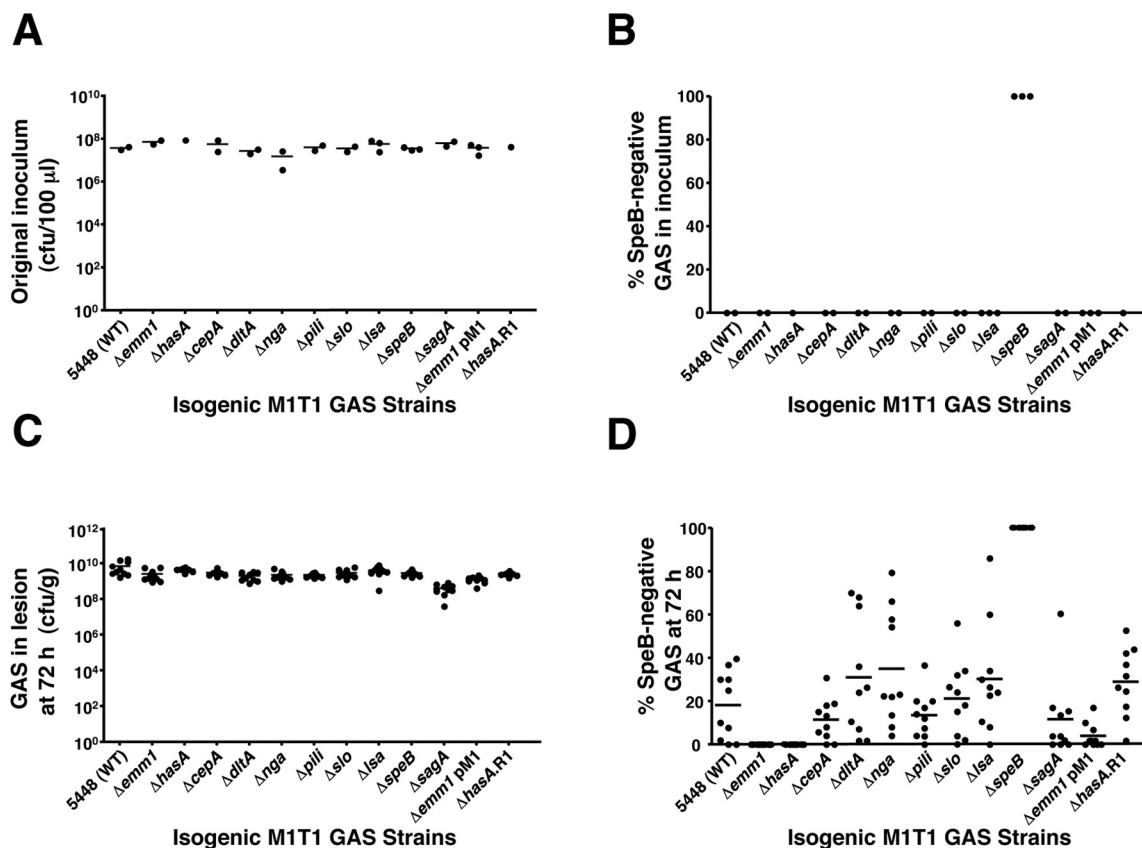


FIG 1 M protein and hyaluronic acid capsule are indispensable for *in vivo* selection of the *covRS* mutant phenotype in GAS serotype M1T1. (A) Quantification of nonlethal inoculum administered to mice subcutaneously. Each symbol shows the value for an individual mouse. The short horizontal bar denotes the arithmetic mean. (B) Percentage of WT and isogenic mutant colonies negative for SpeB protease activity in the original inoculum ($n = 50$). (C) Bacterial load per gram/tissue in harvested skin lesions ($n = 10$) 3 days after subcutaneous infection. (D) Percentage of SpeB-negative colonies in skin lesion after 72 h (10 mice per strain and 50 colonies tested per animal). Each symbol shows the value for an individual mouse. The short horizontal bar denotes the arithmetic mean for each group or strain.

tion was to determine whether other established GAS virulence factors, each found to contribute to neutrophil resistance and/or disease in small animal models, were themselves essential contributors to the M1T1 switch to hypervirulence. A panel of 10 isogenic mutants harboring precise virulence gene mutations were surveyed for SpeB expression status following *in vivo* selection. After surveying these 10 mutants, we report that two GAS virulence determinants, M1 protein and hyaluronic acid capsule, are essential for the *in vivo* selection of *covRS* mutations, whereas the individual deletion of several other virulence factors did not influence this propensity. Furthermore, we demonstrate that hyaluronic acid capsule, like the Sda1 DNase and M1 protein (12), mediates resistance to bacterial clearance within NETs, likely through inhibition of cathelicidin antimicrobial peptides. These data suggest that a specific coordinated subset of GAS serotype M1T1 neutrophil survival factors is required for *in vivo* phase-switching and hypervirulence.

RESULTS

Effect of virulence gene deletion on GAS serotype M1T1 *in vivo* phase-switching. To assess the *in vivo* phase-switch of SpeB during infection, mice were subcutaneously infected with non-lethal doses of wild-type (WT) GAS serotype M1T1 strain 5448

and a panel of 10 isogenic virulence gene mutants derived from this strain. The bacteria in the inocula were counted to confirm that equivalent doses were administered for all strains (Fig. 1A). The WT and mutant inocula were uniformly positive for SpeB proteolytic activity (50 colonies), with the exception of the 5448 Δ speB negative control (Fig. 1B). At 72 h postinfection, bacterial counts within the skin lesions were comparable for WT and mutant strains (Fig. 1C). For each bacterial strain, 50 colonies derived from the lesions of 10 separate mice (500 total) were screened for loss of SpeB activity indicative of *covRS* mutation. GAS serotype M1T1 mutants lacking streptolysin O (5448 Δ slo) (13), streptolysin S (5448 Δ sagA) (14), pilus T1 antigen (5448 Δ pili) (15), interleukin 8 (IL-8) protease SpyCEP (5448 Δ cepA) (16), NAD glycohydrolase (5448 Δ nga) (13), D-alanylation of teichoic acids (5448 Δ dltA) (17), and large surface-anchored (Lsa) antigen (5448 Δ lsa) (18) (also known as extracellular protein factor [Epf]) all demonstrated a clear ability to switch to the SpeB-negative *covRS* mutant phenotype *in vivo*, albeit with somewhat differing efficiencies compared to the WT (Fig. 1D). In contrast, phase-switching associated with loss of SpeB expression *in vivo* was completely abrogated in isogenic GAS mutants lacking M1 protein (5448 Δ emm1) or hyaluronic acid capsule (5448 Δ hasA) (Fig. 1D). Upon comple-

TABLE 1 DNA sequence analyses of mutations within *covRS* genes^a

GAS strain	Mouse ID no. ^b	Mutation ^c
5448	1	G-to-T mutation at nt 1441 in <i>covS</i>
5448	2	A insertion at nt 803 in <i>covS</i>
5448 Δ <i>cepA</i>	1	C-to-T mutation at nt 1363 in <i>covS</i>
5448 Δ <i>cepA</i>	2	T-to-C mutation at nt 866 in <i>covS</i>
5448 Δ <i>dltA</i>	1	A-to-G mutation at nt 278 in <i>covR</i>
5448 Δ <i>dltA</i>	2	C-to-T mutation at nt 889 in <i>covS</i>
5448 Δ <i>nga</i>	1	AAAGG insertion at nt 867 in <i>covS</i>
5448 Δ <i>nga</i>	2	TTTTTT insertion at nt 76 in <i>covS</i> C insertion at nt 77 in <i>covS</i> GCA insertion at nt 78 in <i>covS</i> C insertion at nt 82 in <i>covS</i>
5448 Δ <i>pili</i>	1	C-to-T mutation at nt 1003 in <i>covS</i>
5448 Δ <i>pili</i>	2	TTTTTT insertion at nt 76 in <i>covS</i> C insertion at nt 77 in <i>covS</i> GCA insertion at nt 78 in <i>covS</i> C insertion at nt 82 in <i>covS</i>
5448 Δ <i>slo</i>	1	T insertion at nt 1409 in <i>covS</i>
5448 Δ <i>slo</i>	2	T deletion at nt 213 in <i>covS</i>
5448 Δ <i>lsa</i>	1	G-to-A mutation at nt 1189 in <i>covS</i>
5448 Δ <i>lsa</i>	2	C insertion at nt 137 in <i>covS</i>
5448 Δ <i>sagA</i>	1	C-to-T mutation at nt 761 in <i>covS</i>
5448 Δ <i>sagA</i>	2	C-to-T mutation at nt 761 in <i>covS</i>
5448 Δ <i>emm1</i> pM1	1	C-to-T mutation at nt 352 in <i>covR</i>
5448 Δ <i>emm1</i> pM1	2	C-to-A mutation at nt 608 in <i>covS</i>
5448 Δ <i>hasA</i> .R1	1	G insertion at nt 1374 in <i>covS</i>
5448 Δ <i>hasA</i> .R1	2	G insertion at nt 1374 in <i>covS</i>

^a GAS serotype M1T1 strain 5448 colonies that were derived from lesions and SpeB-negative isogenic colonies isolated 3 days after subcutaneous infection of C57BL/6J mice with nonlethal challenge doses.

^b Mouse identification (ID) number.

^c Mutation positions are based upon the nucleotide (nt) position in the *covR* or *covS* gene relative to each ATG start codon.

mentation of mutant strain 5448 Δ *emm1* with a plasmid expressing M1 protein (pM1) or restoration of the *hasA* allele within a plasmid excisional revertant of mutant strain 5448 Δ *hasA* (5448 Δ *hasA*.R1), the capacity of each mutant to switch to a SpeB-negative phenotype was restored (Fig. 1D). DNA sequence analysis of several SpeB-negative lesion-derived colonies identified mutations within the *covRS* locus (Table 1), consistent with previous studies (5, 6, 9). These data indicate an essential role for M protein and capsule in GAS serotype

M1T1 *in vivo* phase-switching, analogous to that previously identified for the Sda1 DNase (6).

Neutrophil survival. The Sda1 DNase contributes to GAS virulence by degrading NETs, thus allowing the pathogen to escape neutrophil extracellular killing (7, 8). Recently, we demonstrated that M1 protein stimulates NET formation yet also promotes GAS serotype M1T1 bacterial survival within these DNA-based innate defense structures by conferring resistance to cathelicidin antimicrobial peptides (12). To pursue this linkage, we examined how the hyaluronic acid capsule, the third identified contributor to *covRS* phase-switching *in vivo*, contributed to GAS serotype M1T1 neutrophil and NET resistance. Enzyme-linked immunosorbent assay (ELISA) results demonstrated that hyaluronic acid was absent in the 5448 Δ *hasA* mutant and restored to the WT level in the 5448 Δ *hasA*.R1 revertant strain (Fig. 2A). Compared to the WT parent and revertant strains, the acapsular 5448 Δ *hasA* mutant was more sensitive to total neutrophil-mediated killing (Fig. 2B). To isolate extracellular neutrophil killing, the assays were repeated in the presence of cytochalasin D, an actin cytoskeleton inhibitor that blocks phagocytosis. As an assay control, extracellular killing of strain 5448AP (Fig. 2C), the SpeB-negative *covS* mutant that expresses high levels of the NET-degrading Sda1 DNase (6), was greatly diminished. We found that the acapsular 5448 Δ *hasA* mutant exhibited a small but significant reduction in survival compared to the WT and revertant strains (Fig. 2C), indicating that hyaluronic acid capsule expression contributes to GAS resistance to extracellular neutrophil killing, a phenomenon generally attributable to entrapment and/or killing within NETs (19, 20).

NET induction and entrapment. In contrast to M1 protein, which is necessary and sufficient to promote the induction of NETs (12), no significant differences were found in the levels of NETs induced by the WT, hyaluronic acid capsule mutant, or revertant strains (Fig. 3A). Similarly, the absence of capsule did not affect bacterial entrapment within DNA NETs (Fig. 3B). Together these data show that GAS serotype M1T1 capsule does not enhance neutrophil survival by reducing NET induction or entrapment within these structures.

Survival within NETs and cathelicidin resistance. Immunofluorescence microscopy of NET-entrapped GAS using the Live/Dead BacLight bacterial viability kit revealed a markedly higher proportion of dead cells for the acapsular 5448 Δ *hasA* mutant compared to either the WT parent strain or revertant strain 5448 Δ *hasA*.R1 (Fig. 4A). These findings indicate that as found for the M1 protein (12), hyaluronic acid capsule contributes to GAS serotype M1T1 survival within NETs. Cathelicidin antimicrobial peptides are important effectors of bacterial killing within NETs (20, 21), and inhibition of human cathelicidin LL-37 is a key factor by which M1 protein promotes NET resistance (12). We found that the MIC of LL-37 for the 5448 Δ *hasA* mutant was 2-fold lower than that calculated for the WT or revertant strains in both logarithmic and stationary growth phases (Fig. 4B). The enhanced susceptibility to LL-37 of the 5448 Δ *hasA* mutant was confirmed in kinetic killing assays (Fig. 4C).

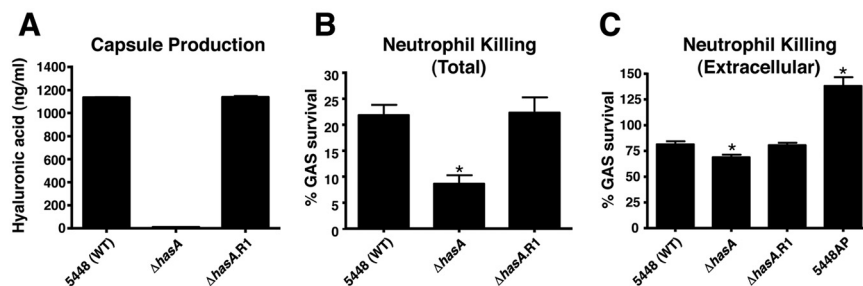


FIG 2 Capsule promotes resistance to neutrophil-mediated killing of GAS serotype M1T1. (A) Capsular hyaluronic acid quantification. Values denote arithmetic means plus standard errors (SEs) (error bars) and are representative of two independent experiments performed in triplicate. (B) Bacterial survival in total (intracellular plus extracellular) neutrophil killing assays. Values represent arithmetic means plus SEs and are representative of three independent experiments performed in triplicate. (C) Survival in extracellular neutrophil killing assays when phagocytic uptake is inhibited with cytochalasin D (10 μ g/ml). Values denote arithmetic means plus SEs and are representative of three independent experiments performed in triplicate. Values that are statistically significantly different ($P < 0.05$) from the value for isolate 5448 (wild type [WT]) are indicated by an asterisk.

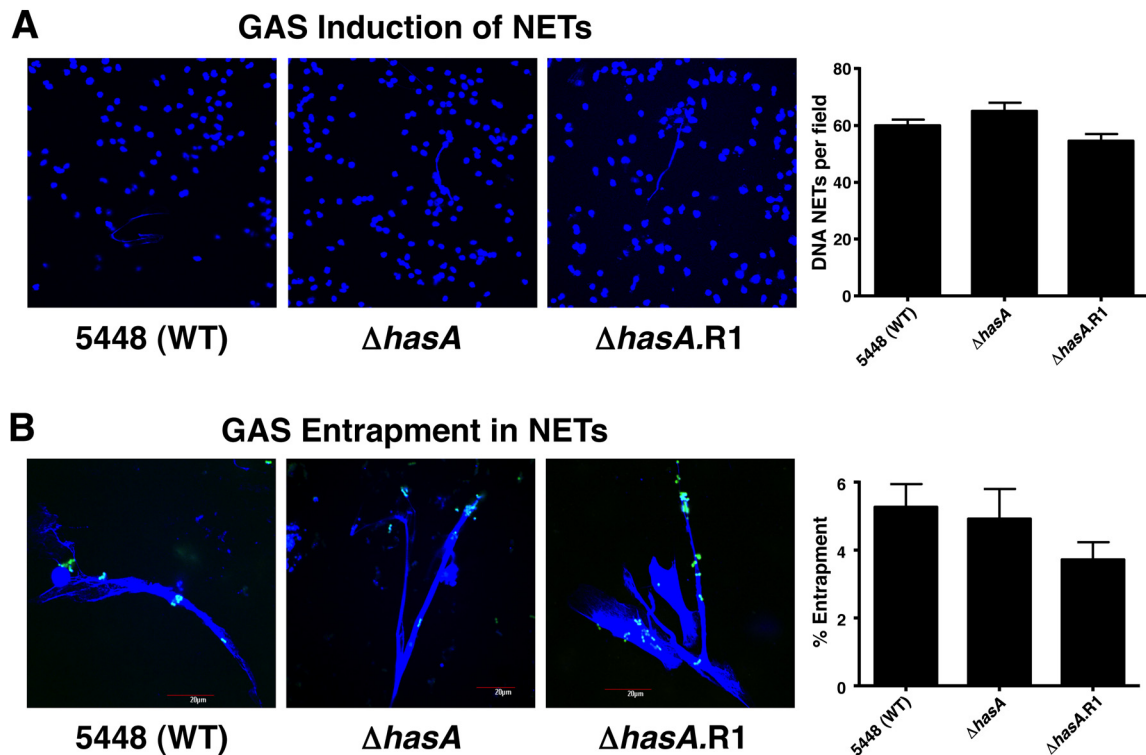


FIG 3 Hyaluronic acid capsule expression does not significantly influence GAS induction of, nor entrapment within, neutrophil extracellular traps (NETs). (A) DAPI-stained DNA NETs (blue) induced by WT GAS serotype M1T1 strain 5448, capsule-deficient mutant 5448 $\Delta hasA$, and revertant 5448 $\Delta hasA.R1$. Fluorescent images are representative of three independent experiments. The bar graph shows quantification of DNA NET induction per field of view after exposure to Sytox Orange. Values denote arithmetic means plus SEs (error bars) and are representative of three independent experiments performed in triplicate. (B) Entrapment of FITC-labeled bacteria (green) within DAPI-stained DNA NETs (blue) for WT GAS serotype M1T1 strain 5448, capsule-deficient mutant 5448 $\Delta hasA$, and revertant 5448 $\Delta hasA.R1$. Fluorescent images are representative of three independent experiments. The bar graph shows quantification of FITC-labeled GAS trapped within DNA NETs by spectrofluorometry. Values denote arithmetic means plus SEs and are representative of two independent experiments performed in triplicate.

Thus, hyaluronic acid expression promotes GAS serotype M1T1 cathelicidin resistance and NET survival, which may account for its essential role in promoting the *covRS* phase-switching mutation to hypervirulence in this globally disseminated epidemic strain.

DISCUSSION

The switch to a hyperinvasive GAS serotype M1T1 phenotype *in vivo* occurs by mutation within *covRS*, which acts to shut off cysteine protease SpeB production while upregulating the expression of several other known GAS virulence factors, including hyaluronic acid capsule, streptolysin O (SLO), NAD glycohydrolase, SpyCEP, and the Sda1 DNase (5). Previously, we reported that expression of the bacteriophage-encoded Sda1, which promotes GAS neutrophil resistance by degradation of NETs (7, 8), was required for the *covRS* switching phenotype (6). Mutations in *covRS* were not detected when the $\Delta sda1$ mutant was used to challenge mice subcutaneously, and an ancestral M1 GAS strain, lacking the phage $\Phi M1T1Z$ encoding Sda1, also failed to switch *in vivo* (6). Here, we examined whether the loss of any other individual GAS virulence factors would be sufficient, in and of itself, to block the selective pressure favoring the *covRS* switching phenomenon *in vivo*. From a panel of 10 isogenic mutants tested, we found that only hyaluronic acid capsule and M1 protein shared with Sda1 an essentiality for the *covRS* switching phenotype.

For a number of GAS serotype M1T1 virulence factors with established or proposed roles in resistance to neutrophil killing, targeted deletion of the gene encoding the virulence factor did not eliminate *covRS* switching *in vivo*. The SpyCEP peptidase degrades the key human CXC chemokine (chemokine with the C-X-C motif) IL-8 to impair directed neutrophil migration and bacterial killing (16, 22), yet *covRS* switching of the GAS $\Delta cepA$ mutant was still readily detected. GAS promotes the accelerated cell death of neutrophils and macrophages through the action of its pore-forming toxins streptolysin S (SLS) and streptolysin O (SLO) (13, 14, 23, 24), but loss of either toxin did not eliminate the *covRS* switching propensity. Likewise, deletion of the surface-anchored protein Lsa (aka Epf) (18, 25), the largest protein encoded by a gene in the serotype M1T1 genome, pilus subunit Spy1028 (15), the building block for the recently discovered fibrillar GAS surface appendages (26), or the NAD glycohydrolase which enhances GAS cytotoxicity through depletion of host intracellular energy stores (27, 28), did not eliminate *covRS* switching. The data indicate that a GAS strain lacking any one of these components nevertheless will experience enhanced survival at the site of infection through *covRS* mutation, such that the selective pressure favoring the *in vivo* mutation for the WT parent strain is retained.

GAS lacking M1 protein ($\Delta emm1$) did not undergo detectable levels of *covRS* mutation *in vivo*. The specificity of this phenome-

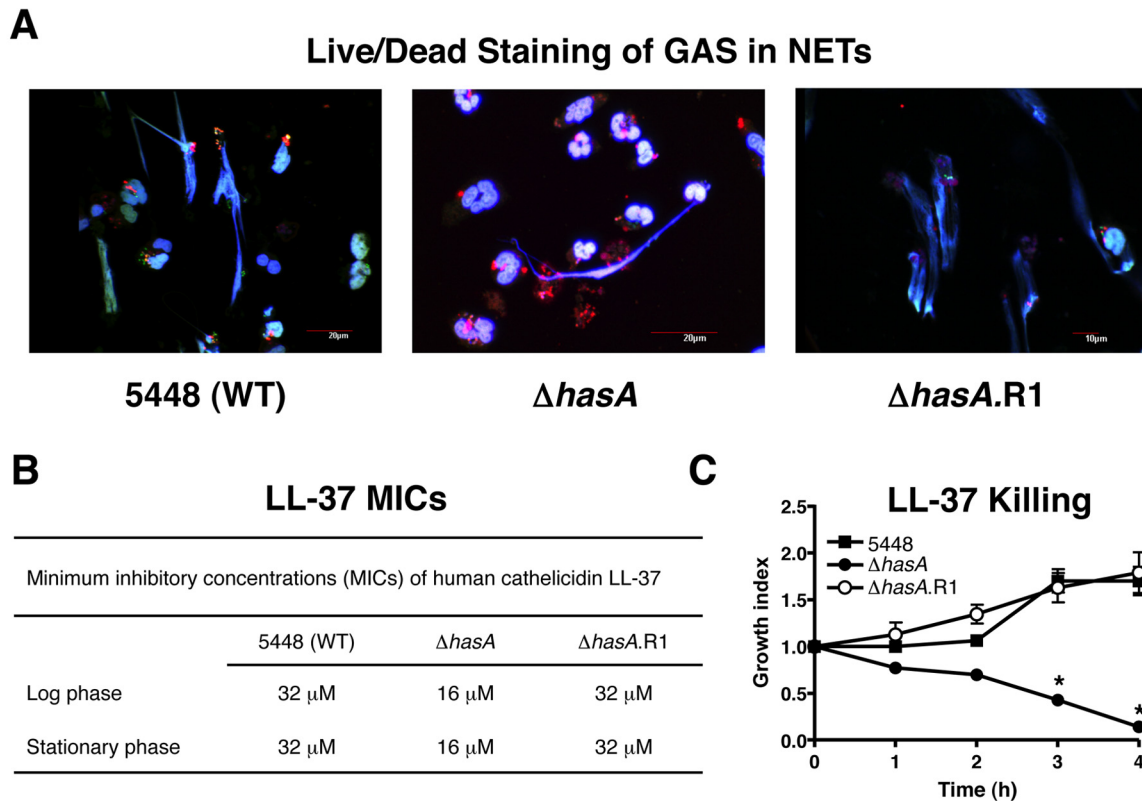


FIG 4 Capsule enhances GAS serotype M1T1 survival within extracellular traps and resistance to human cathelicidin LL-37. (A) Immunofluorescence microscopic overlay images of viable bacteria (green) versus dead bacteria (red) entrapped within DAPI-stained NETs (blue) for WT GAS serotype M1T1 strain 5448, capsule-deficient mutant strain 5448 Δ hasA, and revertant strain 5448 Δ hasA.R1. Fluorescent images are representative of three independent experiments. (B) MICs for cathelicidin antimicrobial peptide LL-37 against WT GAS serotype M1T1 strain 5448, capsule-deficient mutant 5448 Δ hasA, and revertant 5448 Δ hasA.R1 in logarithmic and stationary growth phases. (C) Killing kinetics for WT GAS serotype M1T1 strain 5448, capsule-deficient mutant 5448 Δ hasA, and revertant 5448 Δ hasA.R1 in the presence of LL-37 (64 μ M). The growth index was calculated as the number of CFU at the specified time point/number of CFU in the initial inoculum. Values denote arithmetic means \pm SEs (error bars) and are representative of two independent experiments performed in triplicate. Values that are statistically significantly different ($P < 0.05$) from the value for strain 5448 are indicated by an asterisk.

non was confirmed, as a significant level of *covRS* switching was restored when the Δ *emm1* mutant was complemented using a plasmid expressing M1 protein. GAS M proteins are a multifactorial surface-associated GAS virulence factor that interferes with neutrophil opsonophagocytosis through the binding of fibrinogen (29), complement inhibitory factor H (30), C4b-binding protein (31), and immunoglobulin Fc regions (31). GAS M1 protein has also been shown to promote GAS survival within neutrophils by inhibiting azurophilic granule fusion with the phagosome (32). Recently, M1 protein was found to stimulate the production of NETs but promoted GAS survival within these host defense structures, perhaps by increasing GAS resistance to cathelicidin antimicrobial peptides deployed within the NETs (12). Enhanced resistance to NET-based killing is a phenotypic property shared by M1 protein and the Sda1 DNase (6, 7), and we now recognize that both virulence factors are required for the GAS *covRS* switching phenotype *in vivo*. While transcription of the *emm1* gene is not significantly upregulated upon *covRS* mutation as is transcription of the *sdal* gene (5), M1 protein is normally cleaved/degraded by the SpeB protease whose expression is shut off by the *covRS* switch mechanism (10, 33). Thus, sparing M1 protein from SpeB cleavage results in enhanced neutrophil resistance, leading to selection of *covRS* mutants with abolished SpeB expression *in vivo*.

The hyaluronic acid capsule is a linear high-molecular-weight polymer of glucuronic- β -1,3-*N*-acetylglucosamine located on the surfaces of all GAS strains. The capsule, which is encoded by the highly conserved *has* synthase operon (34), is essentially identical to mammalian polysaccharides, and this molecular mimicry enables GAS to avoid detection by the host immune system (2). Acapsular GAS mutants are sensitive to phagocytic killing *in vitro* and have reduced virulence in a murine model of invasive infection compared with the encapsulated WT strain (35, 36). Here, we find that GAS serotype M1T1 capsule-deficient bacteria do not undergo *covRS* switching *in vivo*, but a revertant regains this capacity. Since we have correlated the absence of *covRS* switching in Δ *sdal* and Δ *emm1* mutants with a role in NET resistance for the genes encoding virulence factors, we examined for the first time whether GAS hyaluronic acid capsule contributes to extracellular neutrophil resistance. In contrast to findings with M1 protein (12), GAS capsule did not contribute to NET induction, and in contrast to studies of the pneumococcal polysaccharide capsule (37), GAS capsule did not impair NET entrapment. However, similar to our observations with M1 protein (12), we found that GAS capsule promoted bacterial survival within human NETs and that this phenotype could be correlated to resistance to the human cathelicidin antimicrobial peptide LL-37, a major component and

antimicrobial effector of NETs. Interestingly, exposure of GAS to LL-37 has been reported to lead to *covRS*-mediated upregulation of capsule expression (38); thus, our discovery of a role for capsule in cathelicidin resistance is consistent with a specific adaptive function of this sensing mechanism. Recently, trapping of other host defense peptides, such as human neutrophil alpha-defensin 1 (HNP-1), beta-defensin 1, and lactoferrin before they can reach their cell wall target of action has been proposed as an immune resistance mechanism for capsular polysaccharides of human bacterial pathogens, including *Klebsiella pneumoniae*, *Streptococcus pneumoniae*, and *Pseudomonas aeruginosa* (39, 40).

We found that both M1 protein and capsule promote resistance to human cathelicidin LL-37, which may be an important contributor to the NET resistance phenotype. However, we show in the present study that the GAS $\Delta dltA$ mutant, which exhibits increased anionic surface charge and increased susceptibility to cationic antimicrobial peptides, including cathelicidin (17), still underwent *covRS* switching *in vivo*. Of note, compared to the parent strain, a *Staphylococcus aureus* $\Delta dltA$ mutant was recently shown to have enhanced sensitivity to cathelicidin within the phagolysosome but not to cathelicidin within NETs (41). This suggests that sequestration of cathelicidin (by M1 protein and perhaps hyaluronic acid capsule) may be a more effective phenotype for cathelicidin resistance than charge repulsion within the NET environment.

In sum, our data indicate that the Sda1 nuclease, M1 protein, and hyaluronic acid capsule comprise a quorum of cooperative virulence factors that promote resistance to NET killing at the site of infection and that efficient NET resistance is required for *in vivo* selection of the *covRS* phenotype linked to hypervirulence and the initiation of invasive disease caused by GAS M1T1 serotype. A number of other bona fide GAS virulence factors, while influencing neutrophil resistance and/or virulence in the murine model, do not appear to alter the fundamental *covRS* switching phenotype significantly. This information suggests a certain hierarchy of virulence determinants with respect to this sentinel event in GAS serotype M1T1 disease progression.

MATERIALS AND METHODS

Bacterial strains, media, and culture conditions. Human GAS serotype M1T1 isolate 5448 was isolated from a patient with necrotizing fasciitis and toxic shock (9). The isogenic animal-passaged SpeB-negative variant 5448AP has been described previously (10). The isogenic in-frame allelic exchange knockout mutants 5448 $\Delta cepA$ (16), 5448 $\Delta dltA$ (17), 5448 Δnga (13), 5448 $\Delta emm1$ (12), 5448 Δslo (13), 5448 Δlsa (18), 5448 $\Delta speB$ (10), 5448 $\Delta sagA$ (14), and 5448 $\Delta pili$ (15) have been described previously. The integrational mutant 5448 $\Delta hasA$ was constructed by Hollands et al. (42). Plasmid-based complementation of the 5448 $\Delta emm1$ mutant strain with pDCerm-*emm1*, hereafter designated 5448 $\Delta emm1$ pM1, is described elsewhere (12). All GAS strains were routinely propagated at 37°C on Todd-Hewitt agar (THA) (Difco) or in static liquid cultures of Todd-Hewitt broth (THB). Where appropriate, strains were grown in media supplemented with 2 μ g/ml erythromycin (Em).

DNA techniques. Chromosomal DNA was extracted using the Colony Fast-Screen kit (Epicentre Biotechnologies). PCR was performed under standard conditions using Platinum Blue PCR supermix (Invitrogen), in accordance with the manufacturer's recommendations.

Integrational mutagenesis of *hasA*. The *hasA* gene in GAS strain 5448 was insertionally inactivated as previously described (42), using temperature-sensitive Em^r vector pHY304. Attempts at complementation of the *hasA* gene or the entire *has* operon of the 5448 $\Delta hasA$ mutant with multicopy plasmid vector pDCerm yielded slow-growing transformants,

suggesting toxicity associated with gene overexpression (not shown). Thus, to generate a revertant to the wild-type (WT) phenotype, henceforth designated 5448 $\Delta hasA$.R1, the Em^r 5448 $\Delta hasA$ mutant strain was passaged at 30°C for 2 days in THB without antibiotic selection pressure, prior to plating serial dilutions onto THA and overnight incubation at 37°C. Loss of the integrated plasmid from the mutant 5448 $\Delta hasA$ chromosome was identified by screening single colonies for Em^s phenotype. Restoration of the *hasA* allele was confirmed by the hyaluronic acid capsule assay and by PCR using primer pair HasA-F (5'-AATGTTTCCTTAATAAATAGTGTG-3') and HasA-R (5'-AAAATTACTCCTTCTCTAACT-3').

Hyaluronic acid capsule assay. Capsular hyaluronic acid levels were quantified by the method of Hollands et al. (42), using the hyaluronic acid quantitative test kit (Corgenix), in accordance with the manufacturer's directions.

FITC labeling of bacteria. GAS bacteria were labeled with fluorescein isothiocyanate (FITC) by a modified version of the method of Goldmann et al. (43). Overnight GAS cultures diluted 1:10 into fresh THB were grown to mid-logarithmic phase, centrifuged at 3,220 \times g for 10 min, and then resuspended in phosphate-buffered saline (PBS) to an optical density at 600 nm (OD₆₀₀) of 0.4, corresponding to $\sim 2 \times 10^8$ CFU/ml. Bacteria were incubated in the presence of 0.2 mg/ml FITC for 30 min on ice in the dark, centrifuged at 3,220 \times g for 10 min, washed twice with PBS to remove excess FITC, and resuspended to the original volume in RPMI 1640 medium without phenol red (Invitrogen) but with 2% heat-inactivated human plasma.

Subcutaneous infection. Overnight cultures of GAS diluted 1:10 to a final volume of 10 ml in THB were grown to an OD₆₀₀ of 0.4, corresponding to mid-logarithmic phase and $\sim 2 \times 10^8$ CFU/ml. Following centrifugation at 3,220 \times g for 15 min, bacterial pellets were washed twice with 10 ml PBS and resuspended in a final volume of 1 ml PBS. Separate cohorts ($n = 10$) of 8-week-old female C57BL/6J mice (Charles River Laboratories, Wilmington, MA) were subcutaneously inoculated with a non-lethal dose ($\sim 10^8$ CFU/100 μ l) to examine the *in vivo* phase-switch of SpeB during infection. To calculate the precise dose administered, serial dilutions of inocula were plated onto THA, and the bacteria were enumerated following overnight incubation at 37°C. Single colonies (50 per inoculum) were tested for SpeB proteolytic activity.

Skin lesion harvest and processing. Three days postinfection, mice were euthanized by CO₂ asphyxiation, and excised skin lesions were placed into sterile preweighed 2-ml screw-cap microtubes containing 1 ml sterile PBS and 1-mm zirconia/silica beads (BioSpec Products). After the tubes were weighed to determine lesion mass, bacteria were released from the skin using two 1-min homogenization bursts with a Mini-BeadBeater (BioSpec Products), in accordance with the manufacturer's instructions. Homogenates were placed on ice for 1 min between bursts to prevent overheating. To quantify bacterial load, homogenates were 10-fold serially diluted in PBS, plated onto THA, and counted following overnight incubation at 37°C. Individual lesion-derived colonies ($n = 50$) were assayed for SpeB expression status.

Cysteine protease activity assay. SpeB protease activity in stationary-phase GAS culture supernatants was determined using the azocaseinolytic assay (44) modified for the 96-well plate format. Single colonies were inoculated into wells (each well containing 200 μ l THB) and incubated at 37°C overnight. After the culture was mixed, 20 μ l of the culture was subinoculated into 180 μ l fresh THB and incubated at 37°C overnight. The cultures were mixed, and the plates were centrifuged at 3,220 \times g for 10 min at room temperature. Forty microliters of culture supernatant and 40 μ l of activation buffer (0.1 M sodium acetate [NaAc] [pH 5], 1 mM EDTA, 20 mM dithiothreitol [DTT]) were mixed in the wells of a fresh microtiter plate and incubated for 1 h at 40°C. Following the addition of 80 μ l of 2% azocasein in activation buffer, the plates were placed at 40°C for 1 h. SpeB-positive wells were identified visually by the orange turbidity generated by azocasein lysis in comparison to the THB-only control. Colonies were scored SpeB negative following negative results in consecutive

assays. For all assays, wild-type strain 5448 and mutant 5448 Δ *speB* culture supernatants were included as positive and negative controls, respectively.

***covRS* sequence analysis.** *SpeB*-negative lesion-derived colonies were screened for mutations within the *covRS* locus essentially as previously described (6).

Neutrophil killing assays. Human neutrophils were isolated and purified from venous blood using the Polymorphprep system (Axis-Shield), resuspended in RPMI 1640 medium (Invitrogen) containing 2% autologous heat-inactivated human plasma, and seeded into 96-well plates at 2×10^5 cells/well. GAS bacteria grown to logarithmic phase (OD_{600} of 0.4) in THB were diluted to the desired concentration in RPMI 1640 medium plus 2% heat-inactivated human plasma and then added to neutrophils at a multiplicity of infection of 1:10 (GAS-to-neutrophil ratio). The plates were centrifuged at $500 \times g$ for 10 min and incubated at 37°C in 5% CO_2 for 30 min. The contents of the wells were serially diluted in sterile H_2O for neutrophil lysis and then plated on THA for overnight incubation and enumeration of surviving GAS CFU. Internal control wells without neutrophils were used to determine baseline bacterial counts at the assay endpoints. Percent survival of GAS was calculated as [(CFU/ml experimental well)/(CFU/ml control well)] \times 100. For extracellular killing assays, neutrophils were treated with 10 μ g/ml cytochalasin D (Sigma-Aldrich) to inhibit phagocytosis 10 min prior to infection.

Immunofluorescence assays. Extracellular trap visualization and viability of GAS entrapped within NETs was undertaken using the Live/Dead BacLight bacterial viability and counting kit (Invitrogen) per the manufacturer's directions. Glass coverslips (1.5 oz, 12 mm; Fisher) were placed in 24-well ultralow-attachment cluster plates (Costar) and coated with 100 μ l of 0.01% poly-L-lysine (Sigma). After 10-min incubation at room temperature, the wells were washed twice with PBS and seeded with 5×10^5 human neutrophils in 500 μ l of RPMI 1640 medium plus 2% heat-inactivated human plasma. The cells were infected with logarithmic-phase GAS at a multiplicity of infection of 2:1 (GAS-to-neutrophil ratio), centrifuged at $500 \times g$ for 10 min, and incubated for 20 min at 37°C in the presence of 5% CO_2 . The cells were washed twice with PBS prior to the addition of 200 μ l of dye and incubation in the dark for 15 min at room temperature. Following three PBS washes, cells were fixed by the addition of paraformaldehyde (PFA) to a final concentration of 1% for 5 min and then washed three times with PBS before the coverslips were embedded on microscope slides in 5 μ l of ProLong Gold antifade reagent with 4',6-diamidino-2-phenylindole (DAPI) (Invitrogen). The slides were stored at 4°C in the dark prior to NET visualization using an inverted confocal laser-scanning 2-photon microscope Olympus FluoView FV1000 with FluoView spectral scanning technology (Olympus). Images were obtained using $20\times/0.7$ or $60\times/1.42$ PlanApo objectives.

Quantification of NETs. Human neutrophils were mixed with GAS at a multiplicity of infection of 1:10 (GAS-to-neutrophil ratio) as described above, and Sytox Orange (Molecular Probes) was added to a final concentration of 0.1 μ M. Following centrifugation at $500 \times g$ for 10 min and 5 min of incubation at 37°C in the presence of 5% CO_2 , extracellular traps were visualized using a Zeiss Axiovert 100 inverted fluorescence microscope. Quantification of NETs was determined by counting transects from three independent wells.

NET entrapment assays. Freshly isolated human neutrophils in RPMI 1640 medium without phenol red (Invitrogen) but with 2% autologous heat-inactivated human plasma were seeded at 2×10^5 per well in 96-well plates and incubated with 25 nM phorbol 12-myristate 13-acetate (PMA) for 4 h at 37°C in the presence of 5% CO_2 to maximally induce NETs and eliminate phagocytosis. An equal volume of FITC-labeled bacteria (100 μ l) was added at a multiplicity of infection of 100:1 (GAS-to-neutrophil ratio), followed by centrifugation at $500 \times g$ for 10 min and incubation for 30 min at 37°C in the presence of 5% CO_2 . To remove unbound bacteria, the wells were gently washed twice with 200 μ l of RPMI 1640 medium without phenol red but with 2% heat-inactivated human

plasma, and the entrapped bacteria were measured by reading the absorbance/emission at 485/538 nm using a SpectraMax Gemini XS spectrofluorometer (Molecular Devices). Percent entrapment of GAS was calculated as follows: [(A485/538 experimental well)/(A485/538 control well without neutrophils)] \times 100. Control wells containing serial dilutions of FITC-labeled bacteria were used for standard curve construction and subsequent quantification of entrapped bacteria.

LL-37 MICs and killing assays. Overnight GAS cultures were diluted 1:10 into fresh THB and grown to logarithmic phase (OD_{600} of 0.4). The bacterial culture was diluted 1:2,000 in PBS plus 50% THB (1×10^5 CFU/ml), and 90- μ l portions were added to individual wells of a 96-well plate containing 10 μ l of human cathelicidin antimicrobial peptide LL-37 (AnaSpec, San Jose, CA) serially diluted in distilled H_2O , giving final LL-37 concentrations equal to 64, 32, 16, 8, 4, and 2 μ M. After incubation at 37°C for 24 h, 5 μ l from each well was plated onto THA and incubated overnight. The MIC was defined as the lowest concentration of LL-37 yielding inhibition of bacterial growth on THA. Killing kinetics in the presence of LL-37 (64 μ M) were monitored at designated time points by serial dilution of 25- μ l aliquots, prior to plating onto THA and overnight incubation at 37°C for CFU enumeration. Growth index was calculated as follows: number of recovered CFU/number of initial CFU.

Statistical analyses. Capsular hyaluronic acid levels, neutrophil survival, NET induction and entrapment, and antimicrobial peptide resistance were compared using the Student's *t* test. All statistical tests were performed using GraphPad Prism version 4.02 (GraphPad Software Inc., San Diego, CA). *P* values of <0.05 were considered statistically significant.

Ethics permissions. Permission to collect human blood samples and to isolate neutrophils was approved by the University of California San Diego (UCSD) Human Research Protections Program. Volunteers provided informed consent before blood samples were obtained. All animal experiments were conducted according to the guidelines approved by the UCSD Institutional Animal Use and Care Committee.

ACKNOWLEDGMENTS

This work was supported by National Health and Medical Research Council of Australia grants 514639 (J.N.C.) and 573401 (M.J.W.), U.S. National Institutes of Health grants AI77780 (V.N.) and AI48176 (R.L.G.), and a Department of Employment Science and Technology (Australia) International Science Linkages grant CG001195 (M.J.W., J.N.C., V.N., and A.H.). M.A.P. is supported in part by an institutional training grant to the UCSD Genetics Training Program, T32 GM008666, from the National Institute for General Medical Sciences. M.V.K.-B. was supported by a fellowship from the Deutsche Akademie der Naturforscher Leopoldina (BMBF-LPD 9901/8-187).

We have no competing financial interests.

REFERENCES

- Carapetis, J. R., A. C. Steer, E. K. Mulholland, and M. Weber. 2005. The global burden of group A streptococcal diseases. *Lancet Infect. Dis.* 5:685–694.
- Cunningham, M. W. 2000. Pathogenesis of group A streptococcal infections. *Clin. Microbiol. Rev.* 13:470–511.
- Aziz, R. K., and M. Kotb. 2008. Rise and persistence of global MIT1 clone of *Streptococcus pyogenes*. *Emerg. Infect. Dis.* 14:1511–1517.
- Engleberg, N. C., A. Heath, A. Miller, C. Rivera, and V. J. DiRita. 2001. Spontaneous mutations in the CsrRS two-component regulatory system of *Streptococcus pyogenes* result in enhanced virulence in a murine model of skin and soft tissue infection. *J. Infect. Dis.* 183:1043–1054.
- Sumby, P., A. R. Whitney, E. A. Graviss, F. R. DeLeo, and J. M. Musser. 2006. Genome-wide analysis of group A streptococci reveals a mutation that modulates global phenotype and disease specificity. *PLoS Pathog.* 2:41–49.
- Walker, M. J., A. Hollands, M. L. Sanderson-Smith, J. N. Cole, J. K. Kirk, A. Henningham, J. D. McArthur, K. Dinkla, R. K. Aziz, R. G. Kansal, A. J. Simpson, J. T. Buchanan, G. S. Chhatwal, M. Kotb, and V. Nizet. 2007. DNase Sda1 provides selection pressure for a switch to invasive group A streptococcal infection. *Nat. Med.* 13:981–985.

7. Buchanan, J. T., A. J. Simpson, R. K. Aziz, G. Y. Liu, S. A. Kristian, M. Kotb, J. Feramisco, and V. Nizet. 2006. DNase expression allows the pathogen group A *Streptococcus* to escape killing in neutrophil extracellular traps. *Curr. Biol.* 16:396–400.
8. Sumbly, P., K. D. Barbican, D. J. Gardner, A. R. Whitney, D. M. Welty, R. D. Long, J. R. Bailey, M. J. Parnell, N. P. Hoe, G. G. Adams, F. R. DeLeo, and J. M. Musser. 2005. Extracellular deoxyribonuclease made by group A *Streptococcus* assists pathogenesis by enhancing evasion of the innate immune response. *Proc. Natl. Acad. Sci. U. S. A.* 102:1679–1684.
9. Kansal, R. G., A. McGeer, D. E. Low, A. Norrby-Teglund, and M. Kotb. 2000. Inverse relation between disease severity and expression of the streptococcal cysteine protease, SpeB, among clonal MIT1 isolates recovered from invasive group A streptococcal infection cases. *Infect. Immun.* 68:6362–6369.
10. Aziz, R. K., M. J. Pabst, A. Jeng, R. Kansal, D. E. Low, V. Nizet, and M. Kotb. 2004. Invasive MIT1 group A *Streptococcus* undergoes a phase-shift *in vivo* to prevent proteolytic degradation of multiple virulence factors by SpeB. *Mol. Microbiol.* 51:123–134.
11. Cole, J. N., J. D. McArthur, F. C. McKay, M. L. Sanderson-Smith, A. J. Cork, M. Ranson, M. Rohde, A. Itzek, H. Sun, D. Ginsburg, M. Kotb, V. Nizet, G. S. Chhatwal, and M. J. Walker. 2006. Trigger for group A streptococcal MIT1 invasive disease. *FASEB J.* 20:1745–1747.
12. Lauth, X., von Köckritz-Blickwede, M., C. W. McNamara, S. Myskowsky, A. S. Zinkernagel, B. Beall, P. Ghosh, R. L. Gallo, and V. Nizet. 2009. M1 protein allows group A streptococcal survival in phagocyte extracellular traps through cathelicidin inhibition. *J. Innate Immun.* 1:202–214.
13. Timmer, A. M., J. C. Timmer, M. A. Pence, L. C. Hsu, M. Ghochani, T. G. Frey, M. Karin, G. S. Salvesen, and V. Nizet. 2009. Streptolysin O promotes group A *Streptococcus* immune evasion by accelerated macrophage apoptosis. *J. Biol. Chem.* 284:862–871.
14. Datta, V., S. M. Myskowski, L. A. Kwinn, D. N. Chiem, N. Varki, R. G. Kansal, M. Kotb, and V. Nizet. 2005. Mutational analysis of the group A streptococcal operon encoding streptolysin S and its virulence role in invasive infection. *Mol. Microbiol.* 56:681–695.
15. Crotty Alexander, L. E., H. C. Maisey, A. M. Timmer, S. H. Rooijackers, R. L. Gallo, M. von Köckritz-Blickwede, and V. Nizet. 2010. MIT1 group A streptococcal pili promote epithelial colonization but diminish systemic virulence through neutrophil extracellular entrapment. *J. Mol. Med.* 88:371–381.
16. Zinkernagel, A. S., A. M. Timmer, M. A. Pence, J. B. Locke, J. T. Buchanan, C. E. Turner, I. Mishalian, S. Sriskandan, E. Hanski, and V. Nizet. 2008. The IL-8 protease SpyCEP/ScpC of group A *Streptococcus* promotes resistance to neutrophil killing. *Cell Host Microbe* 4:170–178.
17. Kristian, S. A., V. Datta, C. Weidenmaier, R. Kansal, I. Fedtke, A. Peschel, R. L. Gallo, and V. Nizet. 2005. D-Alanylation of teichoic acids promotes group A *Streptococcus* antimicrobial peptide resistance, neutrophil survival, and epithelial cell invasion. *J. Bacteriol.* 187:6719–6725.
18. Kwinn, L. A., A. Khosravi, R. K. Aziz, A. M. Timmer, K. S. Doran, M. Kotb, and V. Nizet. 2007. Genetic characterization and virulence role of the RALP3/LSA locus upstream of the streptolysin S operon in invasive MIT1 group A *Streptococcus*. *J. Bacteriol.* 189:1322–1329.
19. Brinkmann, V., U. Reichard, C. Goosmann, B. Fauler, Y. Uhlemann, D. S. Weiss, Y. Weinrauch, and A. Zychlinsky. 2004. Neutrophil extracellular traps kill bacteria. *Science* 303:1532–1535.
20. von Köckritz-Blickwede, M., and V. Nizet. 2009. Innate immunity turned inside-out: antimicrobial defense by phagocyte extracellular traps. *J. Mol. Med.* 87:775–783.
21. Brinkmann, V., and A. Zychlinsky. 2007. Beneficial suicide: why neutrophils die to make NETs. *Nat. Rev. Microbiol.* 5:577–582.
22. Hidalgo-Grass, C., I. Mishalian, M. Dan-Goor, I. Belotserkovsky, Y. Eran, V. Nizet, A. Peled, and E. Hanski. 2006. A streptococcal protease that degrades CXC chemokines and impairs bacterial clearance from infected tissues. *EMBO J.* 25:4628–4637.
23. Goldmann, O., I. Sastalla, M. Wos-Oxley, M. Rohde, and E. Medina. 2009. *Streptococcus pyogenes* induces oncosis in macrophages through the activation of an inflammatory programmed cell death pathway. *Cell. Microbiol.* 11:138–155.
24. Sierig, G., C. Cywes, M. R. Wessels, and C. D. Ashbaugh. 2003. Cytotoxic effects of streptolysin O and streptolysin S enhance the virulence of poorly encapsulated group A streptococci. *Infect. Immun.* 71:446–455.
25. Kreikemeyer, B., M. Nakata, T. Köller, H. Hildisch, V. Kourakos, K. Standar, S. Kawabata, M. O. Glocker, and A. Podbielski. 2007. The *Streptococcus pyogenes* serotype M49 Nra-Ralp3 transcriptional regulatory network and its control of virulence factor expression from the novel *eno ralp3 epf sagA* pathogenicity region. *Infect. Immun.* 75:5698–5710.
26. Mora, M., G. Bensi, S. Capo, F. Falugi, C. Zingaretti, A. G. Manetti, T. Maggi, A. R. Taddei, G. Grandi, and J. L. Telford. 2005. Group A *Streptococcus* produce pilus-like structures containing protective antigens and Lancefield T antigens. *Proc. Natl. Acad. Sci. U. S. A.* 102:15641–15646.
27. Bricker, A. L., V. J. Carey, and M. R. Wessels. 2005. Role of NADase in virulence in experimental invasive group A streptococcal infection. *Infect. Immun.* 73:6562–6566.
28. Michos, A., I. Gryllos, A. Håkansson, A. Srivastava, E. Kokkotou, and M. R. Wessels. 2006. Enhancement of streptolysin O activity and intrinsic cytotoxic effects of the group A streptococcal toxin, NAD-glycohydrolase. *J. Biol. Chem.* 281:8216–8223.
29. Horstmann, R., H. Sievertsen, M. Leippe, and V. Fischetti. 1992. Role of fibrinogen in complement inhibition by streptococcal M protein. *Infect. Immun.* 60:5036–5041.
30. Perez-Casal, J., N. Okada, M. G. Caparon, and J. R. Scott. 1995. Role of the conserved C-repeat region of the M protein of *Streptococcus pyogenes*. *Mol. Microbiol.* 15:907–916.
31. Carlsson, F., K. Berggård, M. Stålhammar-Carlemalm, and G. Lindahl. 2003. Evasion of phagocytosis through cooperation between two ligand-binding regions in *Streptococcus pyogenes* M protein. *J. Exp. Med.* 198:1057–1068.
32. Staali, L., S. Bauer, M. Mörgelin, L. Björck, and H. Tapper. 2006. *Streptococcus pyogenes* bacteria modulate membrane traffic in human neutrophils and selectively inhibit azurophilic granule fusion with phagosomes. *Cell. Microbiol.* 8:690–703.
33. Raeder, R., M. Woischnik, A. Podbielski, and M. D. Boyle. 1998. A secreted streptococcal cysteine protease can cleave a surface-expressed M1 protein and alter the immunoglobulin binding properties. *Res. Microbiol.* 149:539–548.
34. Crater, D. L., and I. van de Rijn. 1995. Hyaluronic acid synthesis operon (*has*) expression in group A streptococci. *J. Biol. Chem.* 270:18452–18458.
35. Moses, A., M. Wessels, K. Zalcman, S. Alberti, S. Natanson-Yaron, T. Menes, and E. Hanski. 1997. Relative contributions of hyaluronic acid capsule and M protein to virulence in a mucoid strain of the group A *Streptococcus*. *Infect. Immun.* 65:64–71.
36. Wessels, M., A. Moses, J. Goldberg, and T. DiCesare. 1991. Hyaluronic acid capsule is a virulence factor for mucoid group A streptococci. *Proc. Natl. Acad. Sci. U. S. A.* 88:8317–8321.
37. Wartha, F., K. Beiter, B. Albiger, J. Fernebro, A. Zychlinsky, S. Normark, and B. Henriques-Normark. 2007. Capsule and D-alanylated lipoteichoic acids protect *Streptococcus pneumoniae* against neutrophil extracellular traps. *Cell. Microbiol.* 9:1162–1171.
38. Gryllos, I., H. J. Tran-Winkler, M. F. Cheng, H. Chung, R. Bolcome III, W. Lu, R. I. Lehrer, and M. R. Wessels. 2008. Induction of group A *Streptococcus* virulence by a human antimicrobial peptide. *Proc. Natl. Acad. Sci. U. S. A.* 105:16755–16760.
39. Campos, M. A., M. A. Vargas, V. Regueiro, C. M. Llopart, S. Alberti, and J. A. Bengoechea. 2004. Capsule polysaccharide mediates bacterial resistance to antimicrobial peptides. *Infect. Immun.* 72:7107–7114.
40. Llobet, E., J. M. Tomás, and J. A. Bengoechea. 2008. Capsule polysaccharide is a bacterial decoy for antimicrobial peptides. *Microbiology* 154:3877–3886.
41. Jann, N. J., M. Schmalzer, S. A. Kristian, K. A. Radek, R. L. Gallo, V. Nizet, A. Peschel, and R. Landmann. 2009. Neutrophil antimicrobial defense against *Staphylococcus aureus* is mediated by phagolysosomal but not extracellular trap-associated cathelicidin. *J. Leukoc. Biol.* 86:1159–1169.
42. Hollands, A., M. A. Pence, A. M. Timmer, S. R. Osvath, L. Turnbull, C. B. Whitchurch, M. J. Walker, and V. Nizet. 2010. A genetic switch to hypervirulence reduces colonization phenotypes of the globally disseminated group A *Streptococcus* MIT1 clone. *J. Infect. Dis.* 202:11–19.
43. Goldmann, O., M. Rohde, G. S. Chhatwal, and E. Medina. 2004. Role of macrophages in host resistance to group A streptococci. *Infect. Immun.* 72:2956–2963.
44. Collin, M., and A. Olsén. 2000. Generation of a mature streptococcal cysteine proteinase is dependent on cell wall-anchored M1 protein. *Mol. Microbiol.* 36:1306–1318.